# Method for the Determination of Myosin Head Orientation from EPR Spectra

Piotr G. Fajer
Institute of Molecular Biophysics and Department of Biological Science, Florida State University, Tallahassee, Florida 32306 USA

ABSTRACT The determination of the iodoacetamide spin label orientation in myosin heads (Fajer, 1994) allows us for the first time to determine directly protein orientation from EPR spectra. Computational simulations have been used to determine the sensitivity of EPR to both torsional and tilting motions of myosin heads. For rigor heads (no nucleotide), we can detect 0.2° changes in the tilt angle and 4° in the torsion of the head. Sensitivity decreases with increasing head disorder, but even in the presence of ±30° disorder as expected for detached heads, 10° changes in the center of the orientational distribution can be detected. We have combined these numerical simulations with a *Simplex* optimization to compare the orientation of intrinsic heads, with the orientation of labeled extrinsic heads that have been infused into unlabeled muscle fibers. The near identity (within 2°) of the orientational distribution in the two instances can be attributed to myosin elasticity taking up the mechanical strain induced by the mismatch of myosin and actin filament periodicity. A similar analysis of the spectra of fibers with ADP bound to myosin revealed a small (~5°–10°) torsional reorientation, without a substantial change of the tilt angle (<2°).

## INTRODUCTION

The movement of the myosin head as proposed by H. E. Huxley (1969) and A. F. Huxley and B. Simmons (1971) has been a cornerstone of the working model for muscle contraction. According to this, and other subsequent models, the binding of myosin heads to actin provokes a conformational change resulting in the development of strain (force), which is relieved by the sliding of actin past the myosin filaments (contraction). The motion of the head, which is the result of the conformational change, could be either axial pivoting, like an oar, ratcheting, as a rack-and-pinion, or lateral sliding if the strain is created outside the myosin head. In the first two scenarios, the head must undergo either tilting or torsional reorientation, whereas in the lateral sliding model the movement of the head is purely translational, and thus more difficult to detect. However, the in vitro assays of Yanagida's and Spudich's groups (reviewed by Burton, 1993) place the force-generating unit within the myosin head and appear to discount the lateral movement model. Much effort has been expended on the description of myosin head orientation, using a variety of structural techniques (Cooke, 1986; Pollard et al., 1993), but the proposed orientational change itself has so far escaped direct detection. In some cases, e.g., electron microscopy, the techniques do not have enough orientational sensitivity; in others (x-ray, optical, and magnetic spectroscopies) interpretation of signals is ambiguous. We used electron paramagnetic resonance spectroscopy (EPR), which is sensitive to the orientation of spin probes attached covalently to myosin heads (Thomas and Cooke, 1980). We previously developed methods to extract the orientational distribution of spins from EPR spectra (Fajer et al., 1990a, b), but until recently, a means of translating probe orientation to the actual protein orientation was not available. The elegant work of Burghardt and Ajtai (1992) attempted to correlate signals originating from different probes, magnetic and optical, to describe protein movement, but does not relate directly the movement to the protein structure. Recently, in an alternative approach, we determined the orientation of the probe within the myosin head, and developed a simulation algorithm explicitly calculating the myosin head orientation within the muscle fiber (Fajer, 1994). This approach takes the interpretation of magnetic resonance spectra one step further, by allowing us to determine myosin head orientation, rather than only probe orientation.

We have used this newly developed method to investigate whether the myosin head is capable of deformation, or whether it behaves as a rigid body. The change of myosin's head shape or orientation during ATP hydrolysis might be responsible for force generation, as postulated by Huxley and Kress (1985). Previously, efforts to observe head shape changes were frustrated by the low resolution of the employed techniques. Neutron scattering studies of isolated heads noted no shape changes (Curmi et al., 1988), whereas some changes were observed in electron micrographs (Tokunaga et al., 1991). The approach taken in the present work is to compare the orientation of the myosin head bound to actin, in the presence and in the absence of constraints due to attachment to the myosin filament. The difference in the periodicities of actin and myosin filaments puts mechanical strain on the head, which, if the head is rigid, will result in a distribution of orientations.

We have also considered the notion of myosin head reorientation induced by the addition of ADP to rigor fibers.

*Received for publication 15 November 1993 and in final form 7 March 1994.*

Address reprint requests to Piotr G. Fajer, Department of Biology, IMB 502, Florida State University, Tallahassee, FL 32306-3015. Tel.: 904-644-7632; Fax: 904-561-1406; E-mail: fajer@irisl.sb.fsu.edu.

*Abbreviations used:* S1, myosin subfragment 1; IASL, perdeuterated *N*-(1-oxy-2,2,6,6-tetratmethyl-4-piperidinyl)iodoacetemide; EPR, electron paramagnetic resonance.



0006-3495/94/06/2039/12 $2.00

The large free energy change associated with the ADP release from myosin has been postulated to result in head movement. The discrepancy between the large reorientation seen with optical probes (Ajtai and Burghardt, 1987) and the much smaller change with spin labels (Fajer et al., 1990b) has been interpreted to be a result of the low sensitivity of spin labels to angular changes (Ajtai and Burghardt, 1986). The high sensitivity to torsional and tilting rotations established in this work contradicts that claim. Small tilting changes (<2°), and somewhat larger (~5°–10°) changes in head torsion, were noted for both extrinsic and intrinsic heads.

## METHODS AND METHODS

### Sample preparation

The myosin head, subfragment-1 (S1) of myosin was prepared by chymotryptic cleavage of myosin according to Weeds and Taylor (1982) with modifications described in Fajer et al. (1988). The purified heads were labeled 100% with perdeuterated iodoacetamide spin label ($^2$H-IASL) synthesized by Dr. Albert Beth of Vanderbilt University. The details of labeling and protein characterization were published previously (Fajer et al., 1988). The labeled heads were infused into bundles of glycerinated muscle fibers treated with Hasselbach-Schneider solution (5 mM MgATP, 0.5 M KPr, 1 mM EGTA, 2 mM $MgCl_2$, 0.5% Triton X-100, 20 mM MOPS pH 7) to remove intrinsic myosin filaments (Yanagida and Oosawa, 1978). The labeling of intrinsic myosin heads was accomplished by the initial preblocking of the reactive sulfhydryls other than Cys-697 and Cys-707, under rigor conditions with 120 $\mu$M DTNB at pH 8.0 in 130 mM KPr, 1 mM EGTA, 2 mM $MgCl_2$, 20 mM MOPS for 120 min on ice (N. Naber and R. Cooke, personal communication). The attachment of the myosin head to actin protects SH-1 and SH-2 from modification by sulfhydryl reagents (Duke et al., 1976). The fibers were then labeled with 0.5 mM $^2$H-IASL in the presence of 5 mM $MgPP_i$ to dissociate the myosin heads from actin and increase the reactivity of Cys-707 (Crowder and Cooke, 1984). The preblocking nitrobenzene group was subsequently removed by thiolysis with 30 mM DTT at 23°C, the efficiency of unblocking (70%) was determined spectrophotometrically. The preblocking, unblocking treatment increases the specificity of labeling, and does not impair any of the actomyosin rate constants as measured by sinusoidal perturbation (Raucher et al., 1993).

### Electron paramagnetic resonance

EPR spectra were obtained in an ESP-106 spectrometer (Bruker Instruments Inc., Billerica, MA) equipped with a modified $TM_{110}$ cavity to allow placement of the muscle fiber bundles (~50 single fibers) parallel to the static magnetic field (Thomas and Cooke, 1980). 21° tilted spectra were obtained by tilting the whole EPR cavity in the magnetic field. To avoid instrumental broadening of the sharp $^2$H-IASL lines, a low microwave field (0.03 Gauss) and a small modulation amplitude (0.2 Gauss) were used in all experiments. The static magnetic field was calibrated with a 0.2 mM peroxylamine disulfonate solution in 50 mM $K_2CO_3$, as described in Faber and Fraenkel (1967), and all spectra were adjusted to the resonance of the secondary field marker, lithium phthalocyanine. The temperature was kept constant at 21°C by a Bruker VT-100 temperature controller. Reproducibility of the spectra from different samples is better than 0.1 Gauss.

### Simulations

Simulations of EPR spectra were accomplished using an Eulerian transformation algorithm, to express the magnetic tensors in the laboratory frame of reference, as described in Fajer (1994). Each Eulerian transformation is defined by a set of three angles $\alpha$, $\beta$, and $\gamma$, which denote torsional reorientation about the $z$ axis, followed by the tilt of the $z$ axis about the newly defined $y$ axis, and the rotation about the tilted $z$ axis, respectively (Fig. 1). We construct three transformations describing (a) probe orientation in the myosin frame of reference, (b) myosin head distribution in the fiber coordinates, and (c) orientation of the fiber with respect to the magnetic field. Each transformation is described by a direction cosine matrix using appropriate Eulerian angles. Angles describing orientation of the probe in the myosin head were recently determined by solving the EPR spectra for samples with the head orientation defined by EM. Two degenerate solutions were found: (16.8°, 28.3°, 4.2°) and (16.6°, 72.0°, 4.3°), and both are used throughout this paper (and Fajer, 1994). The angles refer to the orientation of the IASL probe with respect to the projection of the myosin head in the electron images of decorated actin filaments (Pollard et al., 1993), rather than with respect to the more recently solved 3D structure of the myosin head (Rayment et al., 1993a). The second transformation, the orientation of the myosin head within the fiber, is modeled as a Gaussian centered at $\alpha_o$, with a half-width at half-maximum of $\Delta\alpha$: $\rho(\alpha) = \exp[-\ln 2(\alpha - \alpha_o)^2/(\Delta\alpha)^2]$. A similar expression was used to characterize distribution on $\beta_o$. The angle $\alpha_o$ represents head torsion about the direction defined by the long axis of S1, in the absence of nucleotide, whereas the angle $\beta_o$ represents the head tilt about the perpendicular to the plane of the EM projection. For small torsional angles, $\beta_o$ is a head tilt with respect to the fiber axis. When so defined, angles $\alpha_o$ and $\beta_o$ describe perfectly general positions of the myosin head in space, and are sufficient to describe any head reorientation. The final transformation (fiber-to-laboratory) axis is defined by the experimental setup, the fiber tilt with respect to the magnetic field. Two different fiber tilt angles were used: parallel fiber orientation (tilt = 0°) and an intermediate tilt of 21° (a tilt of 90° does not contribute additional information). The details of the spectral simulations, and the values of the magnetic tensors, are given in Fajer (1994).

### Simplex

The fitting of simulations to experimental spectra, was performed using the *Simplex* algorithm, described in Fajer et al. (1990a). Five spectra are calculated, with different sets of four parameters describing the orientation of the myosin head: $\alpha_o$ and $\beta_o$ and half-width of Gaussian disorder about the average angles $\Delta\alpha$ and $\Delta\beta$ and compared to the experimental spectrum. A four-dimensional *Simplex* figure is constructed with coordinates of the vertices defined by the parameter set, and the value equal to the figure of merit $\chi^2$. The next set of simulation parameters is chosen based on the geometry of the simplex figure. The optimization resembles the crawling of an amoeba on the $\chi^2$ surface towards the lowest minimum (Fajer et al., 1990a). The figure of merit $\chi^2$, describing quality of fit, was defined as the sum of the squared differences normalized to spectral noise and the number of points: $\sum_{i=1}^{Npts}(y_i^{sim} - y_i^{exp})^2/(\text{noise})/\text{Npts}$. Whenever both parallel and 21° tilted fiber were optimized, the head orientation ($\alpha_o$ and $\beta_o$) and disorder ($\Delta\alpha$, $\Delta\beta$) were common to both spectra, and the figure of merit was defined as the sum of $\chi^2$ for each spectrum normalized to the minimum $\chi^2$ for the spectrum in question. This normalization avoids undue weighting of one or the other spectrum. Thus, our optimization strategy has elements of *global analysis,* because two spectra are optimized simultaneously, and elements of *Monte-Carlo methods,* because each optimization is initiated by a random set of parameters, and 50 optimizations are performed in each run.

## RESULTS

### Experimental spectra

The spectra of muscle fibers labeled in situ with $^2$H-IASL (intrinsic heads) and the spectra of labeled S1 decorating unlabeled muscle fibers (extrinsic heads) are shown in Fig. 2. The spectra were taken with the fiber bundle either parallel to the external magnetic field, or inclined at an angle of 21°.

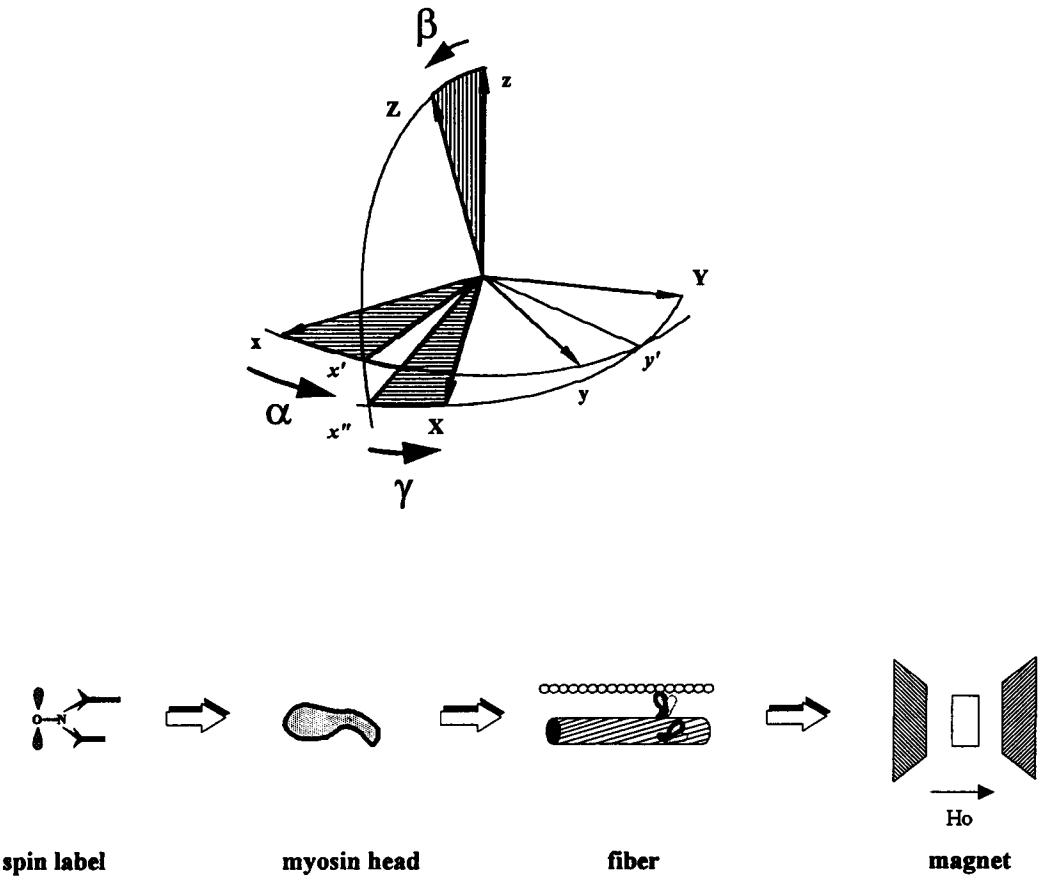


FIGURE 1 Definition of Eulerian angles (*top*) used in the transformations between spin label frame of reference, myosin head, and fiber coordinates (*bottom*).

The muscle was in the absence of any nucleotide (rigor condition) or in the presence of MgADP. The parallel spectra of labeled S1 heads decorating unlabeled fibers are identical to those observed previously for this spin label (Fajer et al., 1990b). They display the characteristic three sharp lines indicative of the high angular order of the principal ($z$-) axis of the spin probe (Thomas and Cooke, 1980). The spectra of intrinsically labeled fibers are almost identical to those of extrinsic heads (see Table 1). This is somewhat surprising considering the mismatch between periodicities of the myosin and actin filaments.

The presence of ADP also does not affect the parallel spectra to a great extent. The splitting, ($2T_{eff}$) becomes slightly smaller (<0.5 Gauss change), and the position of central resonance ($H_c$) changes by <0.3 Gauss. The <3% difference in the lineheight ratios, $L/C$ and $H/C$, indicates no significant change in the width of the Gaussian disorder. In the case of the extrinsically labeled heads, the above differences in ADP have been interpreted as a small (1.3°) reorientation of the $z$ axis of the spin label, with respect to the fiber axis, and an even smaller (0.7°) reorientation of the $x$- and $y$ axis (Fajer et al., 1990b).

The similarities of the 21° tilted fiber spectra further emphasizes the similarity of the orientational distribution. As we have shown previously, partial tilt of oriented fibers decreases ambiguities and spectral degeneracy in the determination of orientational distribution (Fig. 4 in Fajer, 1994).

## Sensitivity of EPR spectra to head reorientation

A description of the orientation of the magnetic tensors, although accurate, does not give direct insight into the behavior of the myosin head. The usual calculations of EPR spectra are based on algorithms expressing the magnetic field direction in polar coordinates, as defined by the magnetic tensor of the label in question. This approach, however, bypasses the orientation of the myosin head. Recently, we applied an alternative algorithm based on Eulerian transformations between probe tensors (IASL), shape of labeled protein (myosin head), assembly of the proteins (muscle fiber), and the laboratory coordinates (direction of the magnetic field); see Fig. 1. An analysis of the spectra of decorated S1, utilizing the head orientation from similar samples as visualized in EM (Pollard et al., 1993), revealed the orientation of the spin probe within the myosin head (Fajer, 1994). Armed with this information, we can explore the relationship between head orientation and the resulting EPR spectra.

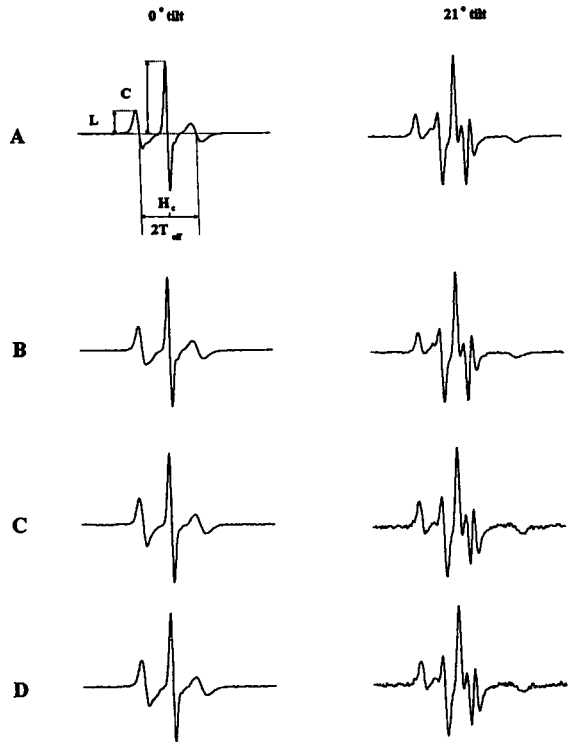


FIGURE 2 EPR spectra of muscle fibers decorated with IASL-labeled myosin heads (*A, C*); fibers with the intrinsic heads labeled (*B, D*) in rigor (*A, B*) and ADP (*C, D*). (*Left*) Spectra of fibers parallel to the magnetic field; (*Right*) fibers tilted at 21° to the magnetic field. Spectra are parametrized in terms of splitting ($2T_{eff}$), center field ($H_c$), and ratio of low-field and center-field peak lineheights ($L/C$) as denoted on the top spectrum.

Fig. 3 shows the dependence of selected spectral parameters (as defined in Fig. 2): (*top*) effective hyperfine splitting, (*middle*) center-field, and (*bottom*) the ratio of low-field and center-field resonance amplitudes, on the myosin head orientation. The angles $\alpha$ and $\beta$ are Eulerian angles relating the the position of myosin head and the long axis of the muscle fiber. The first angle, $\alpha$, represents rotation of the head about its long $z$ axis, followed by a second rotation $\beta$ (tilt of $z$ axis) about the now rotated $y$ axis of the head. The first rotation ($\alpha$) corresponds to the torsion of the head, whereas $\beta$ corresponds to the head tilt in the absence of torsion or combines slew and tilt when torsion is present. To simplify the displays, the simulations shown in Fig. 3 are for well ordered heads with a Gaussian spread of $\pm 6°$ for both head angles. Because there is an ambiguity in the determination of the IASL orientation (Fajer, 1994), both orientations were used in the simulations. These probe orientations are referred here as I (16.8°, 28.3°, 4.2°) and II (16.6°, 72.0°, 4.3°).

Although the behavior of the parameters depends on which of the two probe orientations is used, some generalizations can be made. For instance, it is clear from Fig. 3 that all three spectral parameters are sensitive to both head $\alpha$ and $\beta$ angles. Head torsion ($\alpha$) has its major effect on field center ($H_c$) relative to $T_{eff}$, whereas the head tilt ($\beta$) strongly influences both parameters. The behavior of the $L/C$ ratio is more complex; it is sensitive to head orientation and disorder and should not be taken alone as an indicator of the latter. We stress that the parameters presented in Fig. 3 should not be generalized to any spin label; they are valid only for IASL. Other spin labels oriented at different angles within the head will exhibit different spectral dependence on head orientation.

The sensitivity of spectral lineshape about the rigor orientation ($\alpha_0 = 0°$, $\beta_0 = 40°$) is of particular interest if the head rotates from one position to the rigor orientation during force production. A detailed analysis of $T_{eff}$ and $H_c$ reveals sensitivity to 0.05 Gauss/deg ($\alpha$ angle) and 1 Gauss/deg ($\beta$ angle). As the resolution of EPR spectra is better than 0.2 Gauss, the above sensitivity translates to a resolution of 4° and 0.2° in $\alpha$ and $\beta$, respectively. The angular sensitivity is a function of the head orientation itself with fairly insensitive regions for $\alpha = 57°$–$67°$ if the nitroxide orientation is (16.8°, 28.3°, 4.2°), or $\beta = 12°$–$20°$, for spin label at (16.6°, 72.0°, 4.3°).

Another important aspect of the spectral analysis is the possibility of spectral degeneracy. Are the spectral lineshapes unique, or could two different orientational distributions result in the same spectrum? The isoclinic areas of parameter contour plots in Fig. 3 suggest that identical spectra correspond to different orientational distributions. To search for orientations of the head that might yield identical spectra, we have constructed a grid of fiber simulations as a function of $\alpha$ and $\beta$ and compared each of the simulations to the rigor spectra of fibers decorated with labeled S1. The areas of the quality factor $\chi^2$ between 1 and 3 (all fits between the best and three times worse than the best fits) are shown as a function of head orientation in Fig. 4. Fitting the parallel spectrum results in four and two degenerate areas for probe orientations I and II, respectively. The areas on both plots corresponding to $\alpha_0 = 55°$ can be discounted, because the simulations of fibers tilted at 21° do not fit the corresponding experimental spectra. The remaining area at $\beta_0 = 85°$ for probe orientation I arises from the spectral identity of the heads in opposite halves of a single sarcomere. Although it is unlikely that the proteins will flip by exactly $45° \pm 1°$, we should be aware of this "blind spot" for this particular spin label.

## Sensitivity to head disorder

The above simulations assumed well ordered heads (Gaussian disorder $\Delta\alpha = \Delta\beta = \pm 6°$). Equally important in the contractile cycle are the states in which the head is considerably disordered, e.g., weakly attached states (Fajer et al., 1991a). Therefore, we explored the sensitivity of IASL spectra to increasing disorder of the heads. In the simulations in Fig. 5, rigor head orientation is assumed, and the head's tilt and torsional disorders about this average orientation are varied. Only when the disorder on both angles becomes $\pm 90°$ or greater, the spectra lose their sensitivity to further disorder

**TABLE 1 Selected spectral parameters***

| Sample | State | Fiber tilt (deg) | $2T_{eff}$ (Gauss) | $H_c$ (Gauss) | L/C | H/C |
|---|---|---|---|---|---|---|
| S1 | rigor | 0 | 17.0 | 3488.0 | 0.33 | −0.12 |
| S1 | ADP | 0 | 16.7 | 3488.1 | 0.32 | −0.12 |
| fiber | rigor | 0 | 17.2 | 3487.6 | 0.38 | −0.13 |
| fiber | ADP | 0 | 16.8 | 3487.9 | 0.36 | −0.12 |
| S1 | rigor | 21 | 26.0 | 3484.5 | 0.27 | −0.08 |
| S1 | ADP | 21 | 25.8 | 3484.5 | 0.25 | −0.07 |
| fiber | rigor | 21 | 26.9 | 3484.2 | 0.32 | −0.09 |
| fiber | ADP | 21 | 26.5 | 3484.4 | 0.29 | −0.1 |

* Errors on the field parameters, $2T_{eff}$ and $H_c$, are less than 0.1 Gauss; the errors on lineheight ratios are 10%.

and approach lineshapes characteristic of an isotropic distribution. Such a large disorder places little if any restriction on the orientation of myosin heads with respect to the filament axis. Thus, the EPR spectra remain sensitive to head disorder about the rigor orientation to the limit likely to be imposed by the fiber lattice constraints ($\pm$<90°).

Another question is the sensitivity to reorientation in the presence of large disorder. As an illustration, in Fig. 6 we varied both angles describing head orientation with an assumed disorder of ±30° on both angles. Surprisingly, even for such a large disorder, the spectra remain quite sensitive to torsion and tilt. Their lineshapes are more difficult to parametrize than the spectra of ordered heads; nevertheless, 30° head rotations result in distinct lineshapes, and 10° (on $\beta_o$) can be easily detected.

## Head orientation in muscle fibers

Having established the sensitivity of EPR spectra to the orientational distribution of the myosin heads within a fiber, we can now analyze the S1 distribution in decorated fibers versus the distribution of the intrinsic heads. The extrinsic head is held only by actin, whereas the intrinsic heads are attached to both actin and myosin filaments. The periodicity of these filaments is different; therefore, one might expect intrinsic heads to make different angles with the filament axis, or at least to have a larger spread of orientations, to accommodate varying mechanical strain.

The spectra of fibers with extrinsic and intrinsic labeled heads were analyzed by simultaneous fit of the parallel and 21° tilted spectra, with head orientation ($\alpha_o$ and $\beta_o$) and disorder ($\Delta\alpha$, $\Delta\beta$) as optimization parameters. Fig. 7 shows the best fits to the tilt series using the two probe orientations I and II within the myosin head. The quality of these fits is excellent considering the modeling constraints, i.e., Gaussian distribution on $\alpha_o$ and $\beta_o$. Close inspection reveals that the fits to the parallel spectra are somewhat better, especially in the central region. The parameters of the best fits (shown in Table 2) suggest very small differences in orientational distribution of the intrinsic and extrinsic heads. There is a 2° torsional movement of the heads, accompanied by a 0.3° change in the average tilt angle. The width of the Gaussian distributions remains the same for both cases. The best way of assessing whether these differences are significant, in comparison to the errors introduced by modeling of the distribution as a Gaussian, is to compare the contour plots of the $\chi^2$ at a certain cutoff value denoting bad fits. The plots in Fig. 8 display all areas of the average angles, and the half-width of the Gaussian distribution, which yield fits only half as good as those in Fig. 7, irrespective of probe orientation. This is a very conservative criterion, allowing for the widest reasonable range of possible solutions. A comparison of the areas defining the average position (Fig. 8*A*) shows that even for these relaxed fitting criteria, there is little change in the center of distribution on $\beta_o$. There is, however, a distinct shift of the torsional angle $\alpha_o$ (by at most 6°), reinforcing the conclusion obtained from the best fits. The areas describing head disorder (Fig. 8 *B*) are overlapping: $\Delta\alpha$ = 1°–10° for extrinsic heads and 2°–9° for the intrinsic heads. The corresponding disorder for $\beta_o$ was 3°–6° and 4°–7° for extrinsic and intrinsic heads, respectively. Therefore, we conclude that the orientational distribution of the intrinsic heads in the fiber is nearly the same as the orientation of extrinsic heads in decorated fibers.

## Head orientation in ADP

A similar analysis of $\chi^2$ contours was performed for the fibers in the presence of MgADP. The best fits to both intrinsic and extrinsic heads, in the presence of MgADP, are shown in Fig. 9. The parameters used for these simulations (Table 2) reveal a 2° change in the average tilt angle $\beta_o$, and a ~4°–5° change in $\alpha_o$ for the extrinsic heads. There is also a small ordering effect on head torsion. It should be noted that the orientation of the IASL label within the head does not affect the above conclusions, because the same changes are noted for orientations I and II. Changes of the same order are observed for the labeled fibers, a ~4°–6° change in $\alpha_o$ accompanied by a ~0.7°–1.2° change in $\beta_o$. Relaxation of the fit criteria, to fits that are half-as-good as the best fits, confirms the above findings. The fit areas for decorated fibers in ADP are overlapping those in the absence of nucleotide (Fig. 10), indicating that the observed changes are within the error imposed by the fitting. A larger difference is noted in the case of intrinsically labeled fibers. There is a small, but definite

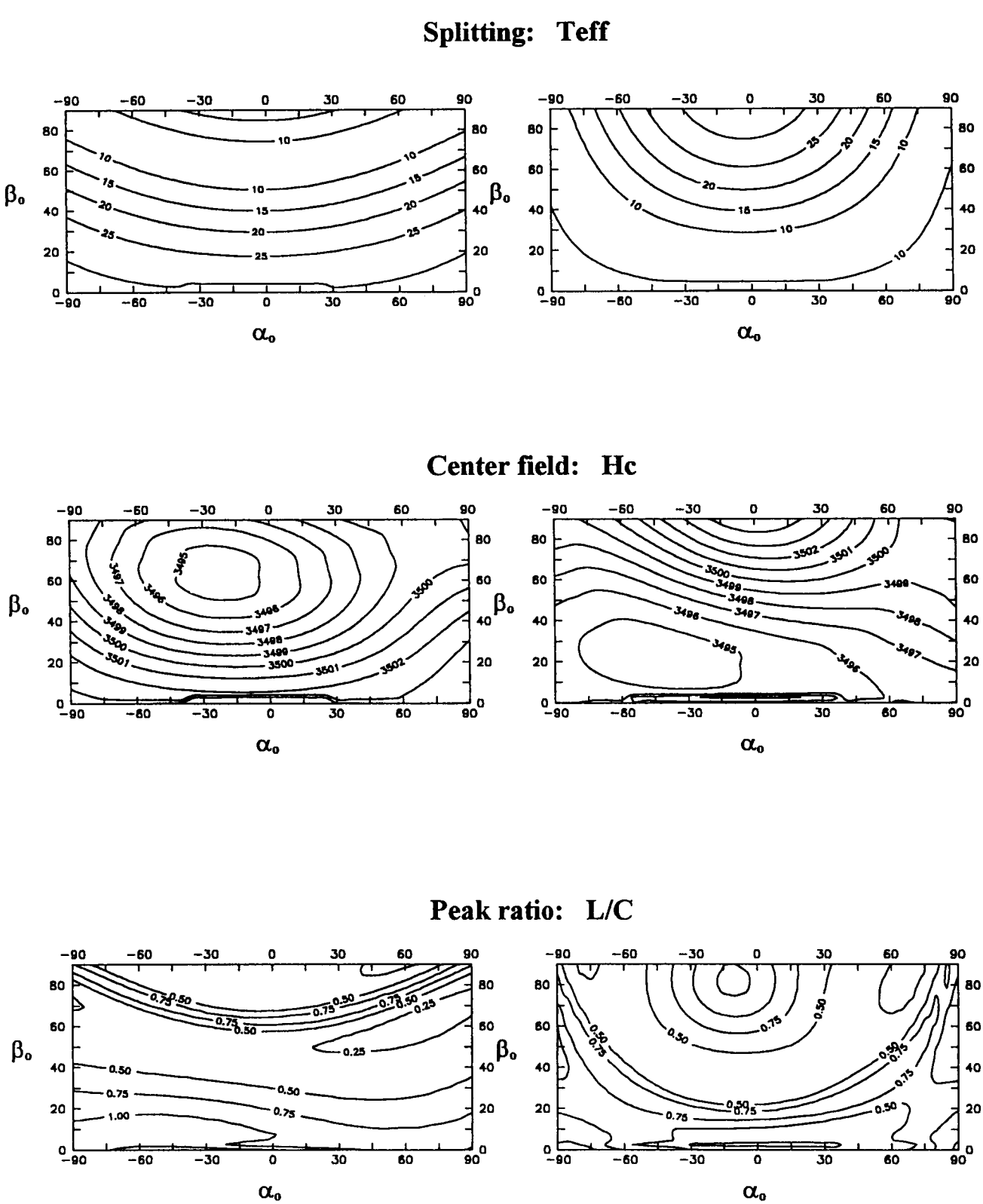


FIGURE 3 The dependence of spectral parameters (defined in Fig. 2) on $\alpha_0$ and $\beta_0$ (the orientation of the myosin head). (*Top*) Splitting ($T_{eff}$); (*middle*) center field ($H_c$) and lineheight (*bottom*) ratio ($L/C$). On the left, spectra are simulated with a probe orientation I of (16.8°, 28.3°, 4.2°), and on the right, a probe orientation II of (16.6°, 72.0°, 4.3°). Head Gaussian disorder is $\Delta\alpha = \Delta\beta = \pm 6°$); (See text for more details.)

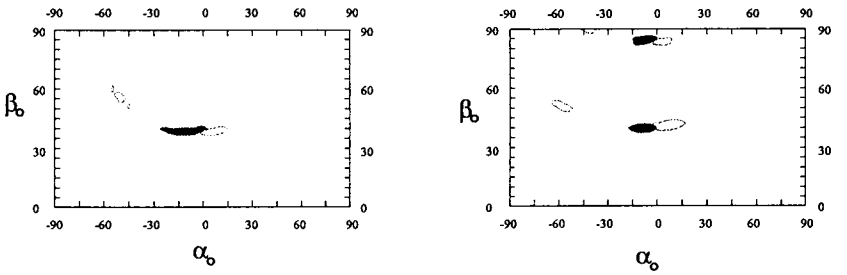


FIGURE 4 Spectral degeneracy of head orientations ($\alpha_o$, $\beta_o$). Contours of $\chi^2$ for grid searches to fit tilt series of rigor spectra to fiber simulations grid: fiber tilt = 0° (*light shade*) and 21° (*filled*) areas. On the left, spectra simulated with probe orientation II, and on the right, probe orientation I. Gaussian disorder is $\Delta\alpha = \Delta\beta = \pm 6°$. Contours correspond to the parameter area for which $\chi^2 = 3\chi^2_{min}$.

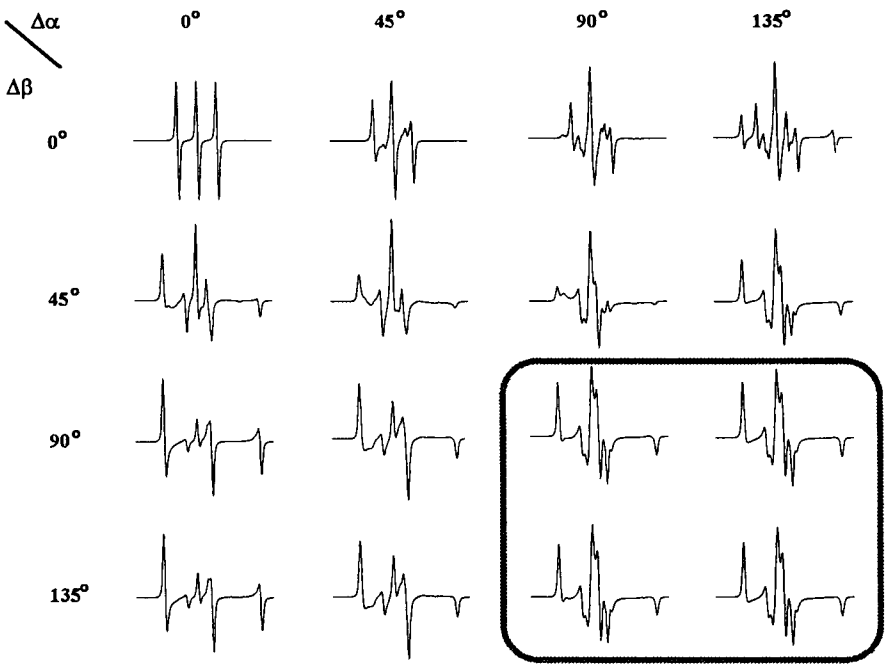


FIGURE 5 EPR spectra of the head oriented as in rigor ($\alpha_o = 0°$, $\beta_o = 40°$) and increasing head disorder. (*Rows*) Increasing in $\Delta\beta$; (*columns*) increasing $\Delta\alpha$. Spin label orientation is (16.6°, 72.0°, 4.3°). Boxed spectra represent limit of spectral sensitivity to orientational disorder.

(~4°–8°), increase of torsional angle in ADP, reflecting the difference obtained from the best fits.

## DISCUSSION

The extraction of myosin head orientation from EPR spectra has been a subject of much effort, since the initial simulations of Thomas and Cooke (1980) were developed for the orientational distribution of spin labels within muscle fibers. Mendelson and Wilson (1982) applied Eulerian angles formalism to consider spin label orientation with respect to the crossbridge, but in the absence of any information about the latter, they were confined to the consideration of arbitrarily chosen label orientations. Our work, very much inspired by these efforts, is in a similar vein, but has the major advantage that the spin label orientation is known (Fajer, 1994).

We have shown that the EPR spectra of heads labeled with IASL are sensitive to the reorientation of the myosin head. For rigor heads and a 0.2 Gauss resolution of EPR spectra, a tilting movement of less than 0.2° can be detected, with a lower (4°) sensitivity to torsional reorientation, if we assume a small head disorder ±6°. This sensitivity is naturally a function of the orientation of the myosin head. When the head is tilted with respect to the fiber, in such a way that the $z$ axis of the nitroxide is perpendicular to the fiber, the sensitivity to the tilt will be at its minimum. This happens for head tilt angles around 60° and 20°, for the two solutions of IASL orientation. For torsional motion, the area of minimum sensitivity is around −20°, at which angle the $x$ axis of the nitroxide is parallel to the fiber. The above estimates, the worst-case scenario, take into account only the behavior of the effective hyperfine splitting ($2T_{eff}$) and the center field ($H_c$), which are the easiest parameters to measure. When the lineheight ratios are included, spectra are sensitive to crossbridge motion at all initial orientations of the head.

We have also established that there is little, if any, orientational degeneracy for the narrow distributions such as in ADP or in the absence of nucleotides. The similarity of the parallel and tilted spectra at $\beta_o = 40°$ and 85° is a reflection of the periodic character of the EPR *Hamiltonian*. It would be a very unlikely coincidence for the myosin head to undergo an exact 45° ± 1° rotation. We can state with reasonable certainty that for narrow EPR spectra, spectral similarity translates into similarity of orientational distributions.

Increasing disorder of the heads decreases the sensitivity of the spectra, but the lineshape remains a function of the tilt and torsion in the presence of disorder as large as ±90°. It is only when the Gaussian disorder on both angles is larger

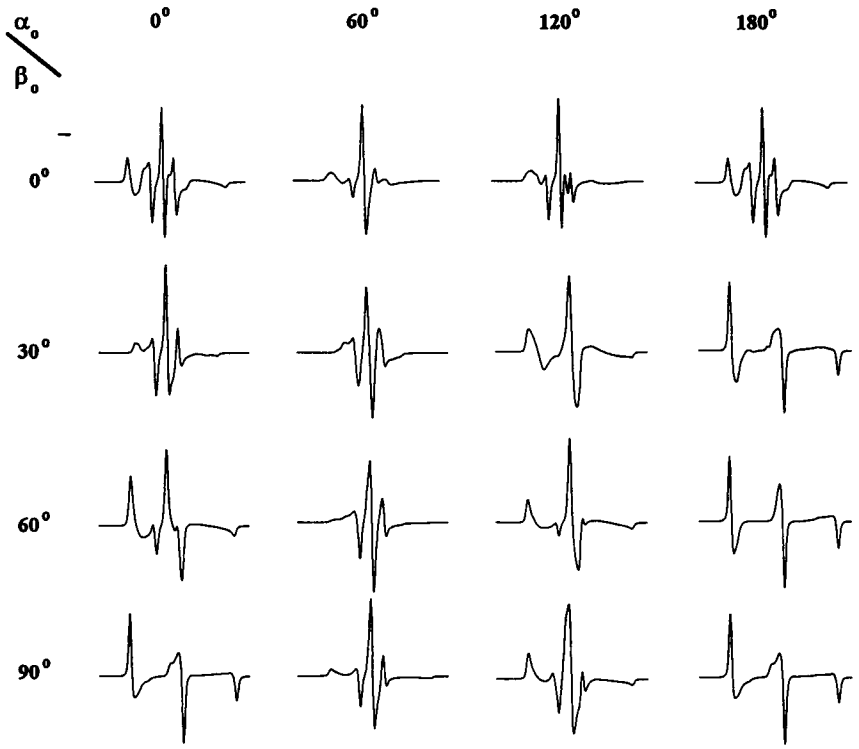


FIGURE 6 Sensitivity of EPR spectra to myosin head reorientation in the presence of large head disorder: $\Delta\alpha = \Delta\beta = \pm 30°$. Other details as in Fig. 5.

than $\pm 90°$ that the spectra approach the isotropic limit. Steric constraints within the fiber lattice limit the width of the head distribution, and $\pm 30°$ disorder is probably a realistic estimate for the upper bound of head disorder. Phosphorescence studies by Thomas and co-workers put a limit of 22° on the amplitude of head motion in relaxation (Stein et al., 1990). Previous warnings (Mendelson and Wilson, 1982) that purely torsional disorder might result in a disordered spectrum for some orientations of the label with respect to the crossbridge are not borne out for the IASL spin label. As seen in Fig. 5, axial Gaussian disorder of at least $\pm 90°$ on both angles is necessary to produce a spectrum approaching an isotropic distribution. Simulations in Fig. 6 document that the spectra are still very sensitive to the head orientation in the presence of large disorder. This demonstrates the feasibility of determining the average orientation of the head, as well as the magnitude of disorder, for states other than those showing well preserved head order. However, we are not suggesting that this will be possible with IASL, because this label is known to undergo rapid librational motion independent of the myosin head, in the presence of ATP (Seidel et al., 1970).

## S1 versus intrinsic heads

Thomas and Cooke (1980) observed that the spectra of spin labels bound to intrinsic myosin heads are very similar to those of the extrinsic heads, implying that the head orientation is similar in both cases. Our contribution is to express these spectral similarities in terms of the myosin head orientational distribution, to analyze quantitatively the difference between intrinsic and extrinsic heads, and to extend the comparison to the ADP state of the myosin head.

The small disorder of extrinsic myosin heads decorating thin filaments in ADP, or in the absence of nucleotide ($\pm 8°$), is in good agreement with the head disorder of $\sim \pm 9° - \pm 13°$ estimated from electron microscopy (Pollard et al., 1993). The absence of substantially larger disorder in the intrinsic heads is somewhat surprising. Some electron micrographs of muscle fibers show a variety of crossbridge angles (Suzuki et al., 1993), and the reconstruction of especially well ordered insect flight muscle implies three different orientations of myosin heads (Taylor et al., 1989). Ignoring possible structural deformation during the preparation of the EM samples, the difference points to the flexibility of the S1 structure. The labeled head domain, which is nearer to the actin binding site than to the hinge region connecting the head and the LMM portion, remains unaffected by the internal strain due to the mismatch of thin and thick filaments. Either the S-2 region of myosin, or the tail of the myosin head, must be accommodating this strain. A similar conclusion was reached when either positive or negative strain along the fiber axis was applied to the crossbridges (Cooke, 1982; Fajer et al., 1991b).

## Myosin head reorientation in MgADP

The addition of ADP to rigor fibers did not result in a large spectral change, either in extrinsic heads decorating fibers or in intrinsic myosin heads. The change of the maximum of ther Gaussian distribution was less than 2° on head tilt and less than 10° on torsion. The width of the distribution was

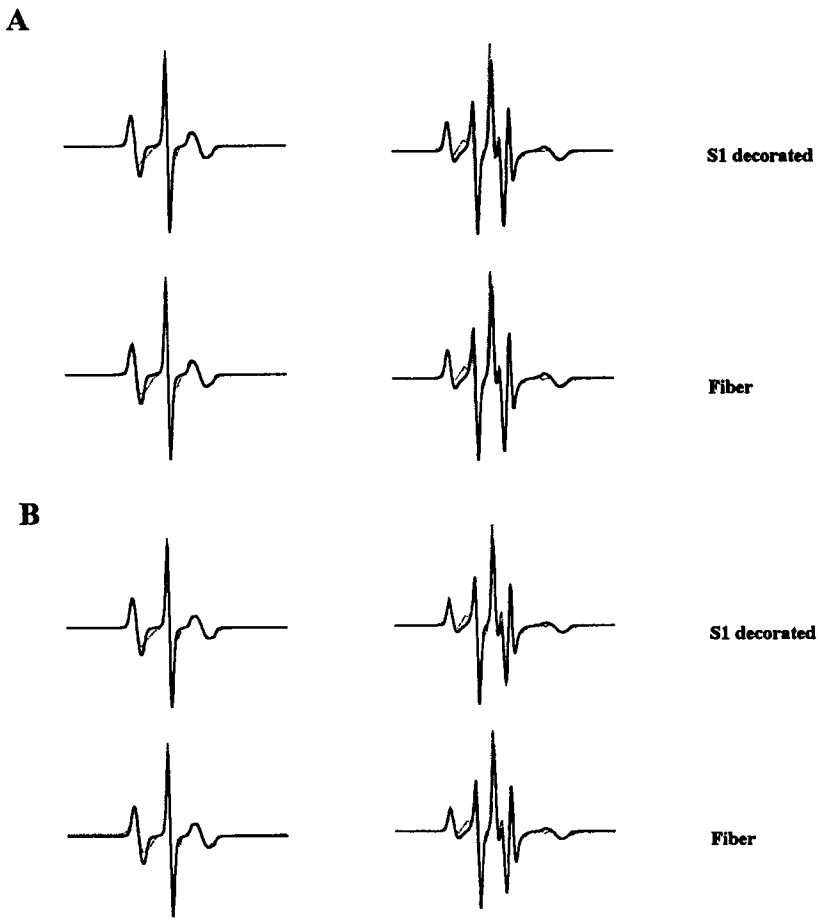


FIGURE 7 Overlays of EPR spectra (*dotted*) and simulated fits (*solid*) of $^2$H-IASL-labeled myosin heads infused into rigor muscle fibers and intrinsically labeled muscle fibers. *Simplex* fits optimized myosin head orientation $\alpha_o$, $\beta_o$, $\Delta\alpha$, $\Delta\beta$. Simulations with spin label orientation I (*A*) and II (*B*).

**TABLE 2 Orientational distribution of myosin heads labeled with IASL**

| Sample | Solution | $\alpha_o$ | $\beta_o$ | $\Delta\alpha$ | $\Delta\beta$ |
|---|---|---|---|---|---|
| IASL orientation I: | | | | | |
| IASL-S1 | Rigor | 0.8 | 40.4 | 6.6 | 5.6 |
| IASL-fiber | Rigor | −1.1 | 40.7 | 5.5 | 5.7 |
| IASL-S1 | MgADP | 4.5 | 42.0 | 4.6 | 5.9 |
| IASL-fiber | MgADP | 2.5 | 41.4 | 5.7 | 6.7 |
| IASL orientation II: | | | | | |
| IASL-S1 | Rigor | 0.9 | 39.6 | 6.9 | 5.4 |
| IASL-fiber | Rigor | −1.5 | 39.0 | 7.8 | 5.5 |
| IASL-S1 | MgADP | 5.7 | 37.6 | 3.5 | 5.7 |
| IASL-fiber | MgADP | 4.6 | 37.8 | 6.9 | 6.7 |

also little affected, although the fits to the ADP spectra were somewhat worse than those of rigor spectra, implying that the Gaussian model describes less well the head distribution in ADP. In view of the small disorder of the heads, as well as the high sensitivity of EPR spectra, we can safely say that the shaded areas in Fig. 10 represent a generous upper limit of the reorientation. We can compare these numbers to those inferred from fiber mechanics. The addition of ADP to rigor muscle fibers results in a 15% decrease of rigor tension. Dantzig et al. (1991) suggested that compliance of the head, in the presence of ADP, is 0.18 nm, as compared to a 12 nm power-stroke. Assuming that the power stroke corresponds to the maximum 45° rotation, from a simple geometric argument one can expect a $40°\text{-}\sin^{-1}[\sin 45°(1–0.18\text{ nm}/12\text{ nm})] = 0.9°$ tilt rotation on the addition of ADP. Although the assumption that the protein undergoes a similar (but smaller) motion, on addition of the ADP as during force generation is an oversimplification, the inferred number compares very well with the observed reorientation.

The absence of large scale reorientation in ADP is in agreement with numerous structural studies such as low-angle x-ray fiber diffraction (Rodger and Tregear, 1984), optical birefringence (Oboriah and Irving, 1989), and electron microscopy (Katayama et al., 1989), but is at variance with the fluorescence probe studies (Ajtai and Burghardt, 1987). Perhaps the various techniques report different aspects of head behavior. Birefringence, microscopy, and x-ray diffraction emphasize global structure of the head, whereas probe studies are sensitive either to local changes in the vicinity of the labeled site, or to global changes, depending on the labeled site and the geometry of the label. Indeed, Thomas pointed out long ago that some EPR probes bound to Cys-707 (e.g., IASL) are sensitive to local conformational changes, whereas others report only global changes (e.g., maleimide spin label), despite being bound to the same site on the myosin head (Thomas, 1987). Not surprisingly, probes attached to different, but nearby, sites can report seemingly contradictory events. A fluorescent probe attached to Cys-697 showed no reorientation on the addition of ADP to fibers,

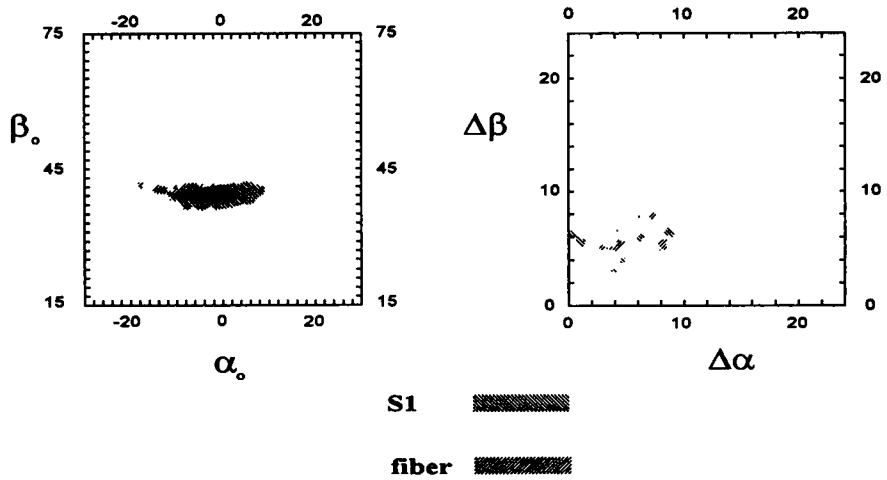


FIGURE 8 Comparison of labeled extrinsic heads infused into fibers and intrinsic heads in labeled fibers. (*Left*) Distribution of average positions $\alpha_o$, $\beta_o$. (*Right*) Gaussian disorder about average position. Contour cutoff at $\chi^2 = 2\chi^2_{min}$.

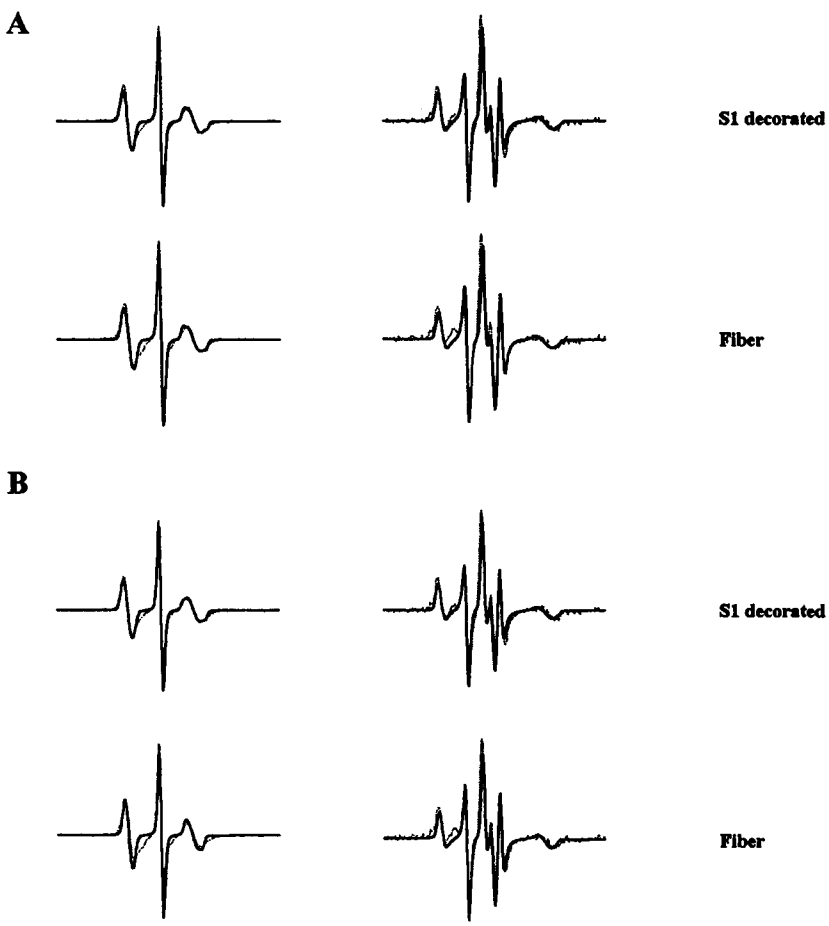


FIGURE 9 Overlays of EPR spectra (*dotted*) and simulated fits (*solid*) of muscle fibers in the presence of 5 mM MgADP: *Simplex* fits optimized myosin head orientation $\alpha_o$, $\beta_o$, $\Delta\alpha$, $\Delta\beta$. Simulations with spin label orientation I (*A*) and II (*B*).

whereas a probe attached to Cys-707 exhibited a change of orientation (Ajtai and Burghardt, 1989). The challenge in probe studies is to determine which signals are to be attributed to global and which to local changes. The correlation of the kinetics of force production with the rate of spectral change clearly showed that, at least in one case, the probe sensed the binding of the nucleotide rather than the structural change responsible for force generation (Tanner et al., 1992).

The recently determined molecular structure of the myosin head points to the root of the problem (Rayment et al., 1993a). Both reactive cysteines of S1 are separated by an $\alpha$-helix near the ATP binding pocket and the cleft in the 50K domain. Rayment postulated that the binding and subsequent hydrolysis of ATP closes the pocket and triggers changes in the cleft region, resulting in the pivoting action of the tail of the myosin head (Rayment et al., 1993b). A similar model

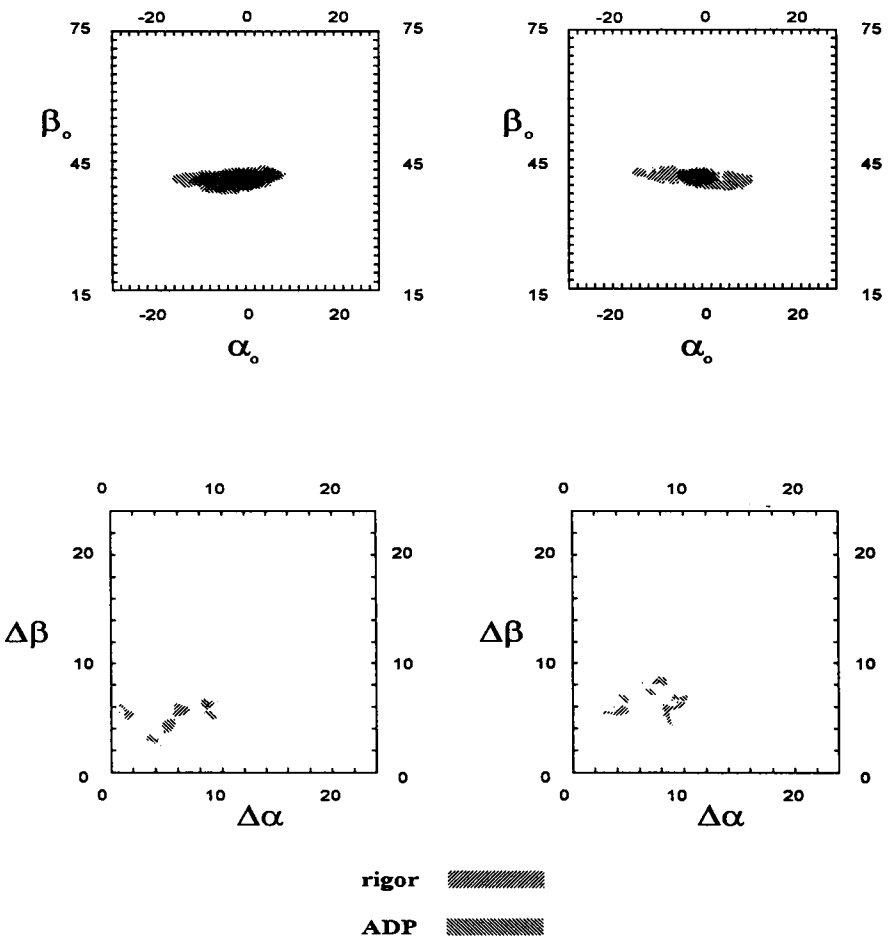


FIGURE 10 Comparison of head orientation in rigor and ADP. Distribution of average positions $\alpha_o$, $\beta_o$ for (*Top left*) S1; (*Top right*) fiber. Gaussian disorder about average position $\Delta\alpha$, $\Delta\beta$: for (*Bottom left*) S1; (*Bottom right*) fiber. Contour cutoff at $\chi^2 = 2\chi^2_{min}$.

was proposed by Highsmith and Eden (1992) to account for the change of the hydrodynamic chord length of S1 on the binding of ADP, as measured by electrical birefringence, and also by Wakabayashi et al. (1992) to explain the same result from small angle x-ray scattering. Depending on where the labeled cysteines are with respect to the pivot point between the proximal and tail portions, the probes might report no movement (proximal side of the pivot), large reorientation (tail side), or be sensitive to local changes if melting of that particular helix accompanies structural changes.

In summary, we have developed computational strategies that are capable of extracting the orientational distribution of labeled myosin heads from EPR spectra. We have successfully applied these methods to rigor myosin heads and also to heads in the presence ADP where we detected a small torsional rotation. The sensitivity to head movement even in the presence of the large disorder as predicted by simulations will allow the determination of head orientation during force generation when the heads are disordered (Fajer et al., 1990c; Hirose et al., 1993).

We thank Roger Cooke and David Thomas for many discussions, and Albert Beth for the gift of perdeuterated IASL. The author is a recipient of an Initial Investigator Award 91II/88 from the American Heart Association.

The support of a National Science Foundation Grant IBN-9206658, and the donation of computing time by the Supercomputer Research Institute at Florida State University, is acknowledged.

## REFERENCES

Ajtai, K., and T. P. Burghardt. 1986. Observation of two orientations from rigor cross-bridges in glycerinated muscle fibers. *Biochemistry.* 25: 6203–6207.

Ajtai, K., and T. P. Burghardt. 1987. Probe studies of the MgADP state of muscle cross-bridges: microscopic and wavelength-dependent fluorescence polarization from 1,5-IAEDANS-labeled myosin subfragment 1 decorating muscle fibers. *Biochemistry.* 26:4517–4523.

Ajtai, K., and T. P. Burghardt. 1989. Fluorescent modification and orientation of myosin sulfhydryl 2 in skeletal muscle fibers. *Biochemistry.* 28:2204–2210.

Burghardt, T. P., and K. Ajtai. 1992. Mapping global angular transitions of proteins in assemblies using multiple extrinsic reporter groups. *Biochemistry.* 31:200–206.

Burton, K. 1992. Myosin step size: estimates from motility assays, and shortening muscle. *J. Muscle Res. Cell Motil.* 13:590–607

Cooke, R. 1981. Stress does not alter the conformation of a domain of the myosin cross-bridge in rigor muscle fibers. *Nature.* 294:570–571.

Cooke, R., 1986. The mechanism of muscle contraction, CRC-Crit-Rev-Biochem, 21:53–118.

Crowder, M. S., and Cooke, R. 1984. The effect of myosin sulphydryl modification on the mechanics of fibre contraction. *J. Muscle Res. Cell Motil.* 5:131–146.

Curmi, P. M. G., D. B. Stone, D. K. Schneider, J. A. Spudich, and R. A.

Mendelson. 1988. Comparison of the structure of myosin subfragment 1 bound to actin and free in solution. A neutron scattering study using actin made "invisible" by deuteration. *J. Mol. Biol.* 203:781–798.

Dantzig, J. A., M. G. Hibberd, D. R. Trentham, and Y. E. Goldman. 1991. Cross-bridge kinetics in the presence of MgADP investigated by photolysis of caged ATP in rabbit PSOAS muscle fibres. *J. Physiol.* 432: 639–680.

Duke, J., R. Takashi, K. Ue, and M. F. Morales. 1976. Reciprocal reactivities of specific thiols when actin binds to myosin. *Proc. Natl. Acad. Sci. USA.* 73:302–306.

Faber, R. J., and G. K. Fraendel. 1967. Dynamic frequency shifts and the effects of molecular motions in the electron spin resonance spectra of dinitrobenzene anion radicals. *J. Chem. Phys.* 47:2462–2467.

Fajer, P. G., E. A. Fajer, N. J. Brunsvold, and D. D. Thomas. 1988. Effects of AMPPNP on the orientation and rotational dynamics of spin-labeled muscle crossbridges. *Biophys. J.* 53:513–524.

Fajer, P., B. Bennett, C. Polnaszek, E. A. Fajer, and D. D. Thomas. 1990a. General method for multiparameter fitting of high-resolution EPR spectra using a *simplex* algorithm. *J. Magn. Res.* 88:111–125.

Fajer, P., E. Fajer, J. Matta, and D. D. Thomas. 1990b. Effect of ADP on the orientation of spin-labeled myosin heads in muscle fibers: a high-resolution study with deuterated spin labels. *Biochemistry.* 29: 5865–5871.

Fajer, P., E. Fajer, and D. D. Thomas. 1990c. Myosin heads have a broad orientational distribution during isometric muscle contraction: time-resolved EPR studies using caged ATP. *Proc. Natl. Acad. Sci. USA.* 87: 5538–5542.

Fajer, P., E. Fajer, Mark Schoenberg, and D. D. Thomas. 1991a. Orientational disorder and motion of weakly attached crossbridges. *Biophys. J.* 60:642–649.

Fajer, P. G., Johnson, P., and Thomas, D. D., 1991b. Head orientation under negative strain. *Biophys. J.* 59:419*a*. (Absrt.)

Fajer, P. G. 1994. Determination of spin label orientation within the myosin head. *Proc. Natl. Acad. Sci. USA.* 91:937–941.

Haselgrove, J. C. 1983. Structure of vertebrate striated muscle as determined by X-ray diffraction studies, Skeletal muscle. *In* Handbook of Physiology. L. D. Peachey, R. H. Adrian, and S. R. Geiger, editors. American Physiological Society, Bethesda, MD. 143–171.

Highsmith, S., and D. Eden. 1990. Ligand-induced myosin subfragment 1 global conformational change. *Biochemistry.* 29:4090.

Hirose, K., T. D. Lenart, J. M. Miurray, C. Franzini-Armstrong, and Y. E. Goldman. 1993. Flash and smash: rapid freezing of muscle fibers activated by photolysis of caged ATP. *Biophys. J.* 65:397–408.

Huxley, A. F., and R. M. Simmons. 1971. Proposed mechanism of force generation in striated muscle. *Nature.* 233:533–538.

Huxley, H. E. 1969. The mechanism of muscle contraction. *Science (Wash. DC).* 164:1356–1366.

Huxley, H. E., and M. Kress. 1985. Crossbridge behaviour during muscle contraction. *J. Muscle Res. Cell Motil.* 6:153–161.

Katayama, E. 1989. The effects of various nucleotides on the structure of actin attached myosin subfragment-2 studied by quick-freeze deep-etch electron microscopy. *J. Biochem. (Tokyo).* 106:751–770.

Mendelson, R. A., and M. G. A. Wilson. 1982. Three-dimensional disorder of dipolar probes in a helical array. Application to muscle cross-bridges. *Biophys. J.* 39:221–227.

Oboriah, O., and M. Irving. 1989. ADP binding to rigor crossbridges produces no major change in their conformation. *Biophys. J.* 55:9*a*. (Abstr.)

Pollard, T. D., D. Bhandari, P. Maupin, Daniel Wachsstock, A. G. Weeds, and H. G. Zot. 1993. Direct visualization by electron microscopy of the weakly bound intermediates in the actomyosin adenosine triphosphatase cycle. *Biophys. J.* 64:454–471.

Raucher, D., E. A. Fajer, K. Hideg, C. P. Sár, Y. Zhao, M. Kawai, and P. G. Fajer. 1993. A non-perturbing spin label for myosin heads. *Biophys. J.* 64:360*a*. (Abstr.)

Rayment, I., H. M. Holden, M. Whittaker, C. B. Yohn, M. Lorenz, K. C. Holmes, and R. A. Milligan. 1993. Structure of the actin-myosin complex and its implications for muscle contraction. *Science.* 261:58–65.

Rayment, I., W. R. Rypniewski, K. Schmidt-Bäse, R. Smith, D. R. Tomchick, M. M. Benning, D. A. Winkelmann, G. Wesenberg, and H. M. Holden. 1993. Three-dimensional structure of myosin subfragment-1: A molecular motor. *Science.* 261:50–58.

Rodger, C. D., and R. T. Tregear. 1974. Letter: crossbridge angle when ADP is bound to myosin. *J. Mol. Biol.* 86:495–497.

Seidel, J. C., M. Chopek, and J. Gergely. 1970. Effect of nucleotides and pyrophosphate on spin label bound to S1 thiol groups of myosin. *Biochemistry.* 54:3265*a*. (Abstr.)

Stein, R. A., R. D. Ludescher, P. S. Dahlberg, P. G. Fajer, R. L. H. Bennett, and D. D. Thomas. 1990. Time-resolved rotational dynamics of phosphorescent-labeled myosin heads in contracting muscle fibers. *Biochemistry.* 29:10023–10031.

Suzuki, S., Y. Oshimi, and H. Sugi. 1993. Freeze-fracture studies on the cross-bridge angle distribution at various states and the thin filament stiffness in single skinned frog muscle fibers. *J. Electron Microsc.* 42: 107–116.

Tanner, J. W., D. D. Thomas, and Y. E. Goldman. 1992. Transients in orientation of a fluorescent cross-bridge probe following photolysis of caged nucleotides in skeletal muscle fibres. *J. Mol. Biol.* 223:185–203.

Taylor, K. A., M. C. Reedy, L. Córdova, and M. K. Reedy. 1989. Three-dimensional image reconstruction of insect flight muscle. I. The rigor myac layer. *J. Cell Biol.* 109:1085–1102.

Thomas, D. D., and R. Cooke. 1980. Orientation of spin-labeled myosin heads in glycerinated muscle fibers. *Biophys. J.* 32:891–906.

Thomas, D. D. 1987. Spectroscopic probes of muscle cross-bridge rotation. *Annu. Rev. Physiol.* 49:691–709.

Tokunaga, M., K. Sutoh, and T. Wakabayashi. 1991. Structure and structural change of the myosin head. *Adv. Biophys.* 27:157–167.

Wakabayashi, K., M. Tokunaga, I. Kohno, Y. Sugimoto, T. Hamanaka, Y. Takezawa, T. Wakabayashi, and Y. Amemiya. 1992. Small-angle synchrotron X-ray scattering reveals distinct shape changes of the myosin head during hydrolysis of ATP. *Science.* 258:443–447.

Weeds, A. G., and R. S. Taylor. 1975. Separation of subfragment-1 isoenzymes from rabbit skeletal muscle myosin. *Nature (Lond.).* 257:54–56.

Yanagida, T., and Oosawa, F. 1978. Polarized fluorescence from e-ADP incorporated into F-actin in a myosin-free single fiber: conformation of F-actin and changes induced in it by heavy meromyosin. *J. Mol. Biol.* 126:507:524